Thermomagnetic properties and magnetocaloric effect of FeCoNiCrAl-type high-entropy alloys

Cite as: AIP Advances 9, 035010 (2019); doi: 10.1063/1.5079394
Presented: 16 January 2019 • Submitted: 30 October 2018 •
Accepted: 5 December 2018 • Published Online: 11 March 2019

Suok-Min Na,[1,a)] Paul K. Lambert,[1] Hyunsoo Kim,[2] Johnpierre Paglione,[2] and Nicholas J. Jones[1]

AFFILIATIONS

[1] Physical Metallurgy and Fire Protection Branch, Naval Surface Warfare Center, Carderock Division, West Bethesda, Maryland 20817, USA
[2] Center for Nanophysics and Advanced Materials, University of Maryland, College Park, Maryland 20742, USA

Note: This paper was presented at the 2019 Joint MMM-Intermag Conference.
[a)] **Corresponding author:** Suok-Min Na, **e-mail address:** suok.na@navy.mil

ABSTRACT

In this work, we investigate the effects of substituting Ni/Al for Cr on the thermomagnetic and magnetocaloric properties of FeCoNiCrAl-type high entropy alloys (HEAs). Ni and Al appear to prefer the BCC phase, and increases in the Al composition appear to stabilize the BCC phase. In contrast to Al, Ni content yields an increase in the FCC phase fraction, resulting in a drop off in magnetization. The phase transformation from BCC to FCC was intensified at annealing temperatures of 800 °C and higher due to increased diffusion rates and the resulting spinodal decomposition. A magnetic phase transition around 150 K was found in the $FeCoNi_{1.5}Cr_{0.5}Al$ annealed alloy potentially corresponding to the FCC phase, and a very broad magnetic phase transition was observed in the annealed FeCoNiCrAl alloy, resulting in a high refrigerant capacity of RC_{FWHM} = 242.6 J·kg^{-1} near room temperature. A peak magnetic entropy change of $-\Delta S_M$ = 0.674 J·kg^{-1}·K^{-1} was also obtained at applied fields of ~70 kOe at 290 K in the FeCoNiCrAl HEA. These magnetocaloric values are comparable to Fe-based metallic glasses such as Fe-Tm-B-Nb and Fe-Zr-B-Co alloys, with a similar transition near room temperature.

I. INTRODUCTION

Magnetocaloric materials have the potential to improve the efficiency of traditional gas compression refrigeration, providing a solid state cooling methodology with no need for environment-harming refrigerants. The challenge, however, is to maintain a high magnetic entropy change over a large temperature range. Giant magnetocaloric materials exhibit very large magnetic entropy changes ($-\Delta S_m$), but over a very narrow temperature band, due to a first-order magneto-structural phase transformation. In addition, the transition temperature of this type of material is often well below room temperature, reducing their applicability to everyday applications. Second order magnetic transitions exhibit a smaller peak value, but over a much wider temperature range. This allows them to operate over a larger temperature range, and their overall performance can be captured by the refrigerant capacity (RC). In a quest to find new allows with a high peak entropy change and a broad temperature transition, many unique classes of materials have been pursued in recent times. High entropy metallic glasses (HEMG) with rare earth (RE) elements exhibit strong topological and chemical disorder, resulting in an enhanced large magnetocaloric effect (MCE) and refrigerant capacity, which are important for improving the efficiency of the refrigerant.[1–5] However, their Curie temperatures (T_C) are much below room temperature (RT), which is unsuitable for ambient temperature applications. On the other hand, RE-free soft magnetic alloys have T_C close to RT, but their MCE is comparatively small.[6–9]

High-entropy alloys (HEAs) are another class of alloys that has gained much popularity in structural, high temperature, and corrosion resistant applications, but can also exhibit beneficial magnetic properties.[10,11] High-entropy alloys generally contain five or more principal elements, which are often found in equiatomic and nearly-equiatomic compositions; in contrast, conventional alloys are generally based on one major element and several minor elements, such as iron in steels.[12] Substituting or adding elements may change the phases present in the annealed sample, as well, which can be predicted for the annealed condition by calculating the valence electron concentration (*VEC*) of the alloy; the resultant phases will also determine the alloy's magnetic properties.[13] In our previous work, the low Curie Temperature (T_C) of FeCoNiCr ($T_C \approx 104$ K) was shifted to room temperature by adding aluminum as a fifth, equiatomic component (FeCoNiCrAl: $T_C \approx 300$ K). In addition, the sharpness of the FeCoNiCr magnetic transition changes drastically by adding Al,[14] exhibiting a gradual and continuous change in magnetization near T_C which is promising for use in magnetic refrigeration.[15]

By altering the composition of RE-free HEAs such as FeCoNiCrAl with T_C near RT, we may therefore be able to define the phases present and tailor the magnetic properties, including MCE, to overcome potential drawbacks. In this work, we systematically investigate the effects of substituting Ni or Al for Cr on the thermomagnetic and magnetocaloric properties of $FeCoNi_{1+X}Cr_{1-X}Al$ and $FeCoNiCr_{1-X}Al_{1+X}$ HEAs with X=0-0.5 (both based on an equiatomic FeCoNiCrAl HEA).

II. EXPERIMENTAL PROCEDURES

Ingots weighing approximately 60 grams with nominal compositions of $FeCoNi_{1+X}Cr_{1-X}Al$ and $FeCoNiCr_{1-X}Al_{1+X}$ (X=0.0, 0.1, 0.2, 0.3, 0.4 and 0.5) were prepared by arc melting under a high purity argon atmosphere. The purity of elements was higher than 99.99 atomic percent (at.%), and the ingots were remelted five times. The ingots were then cut into discs for magnetic measurements at low and room temperatures. Each sample was subsequently annealed at 600, 800, and 1000 °C for 3 hours, then furnace cooled, and tested after each anneal. Slices with thicknesses of ~0.60 mm were cut from each button. From these slices, discs with diameters of ~8.10 and ~6.25 mm were extracted for microstructural analysis and magnetic measurements, respectively.

Magnetic field dependence of magnetization (*M-H*) was measured at RT using a Lakeshore vibrating sample magnetometer (VSM) under applied magnetic fields up to ±20 kOe; applied field values were not corrected for sample shape anisotropy (correction values are small, however, due to the aspect ratio of the disc samples). Temperature dependence of magnetization (*M-T*) was measured in both temperature ranges of 2 – 380 K and 100 – 440 K using a Quantum Design Magnetic Property Measurement System (MPMS XL) and the VSM with a liquid nitrogen (LN_2) cryogenic system, respectively. Energy dispersive x-ray spectroscopy (EDS, EDAX Genesis) was used for collecting compositional data including mapping for each element. X-ray diffraction was performed using a Bruker D8 Advance X-ray Diffractometer (XRD) with LynxEye detector, to determine the crystallographic phases present.

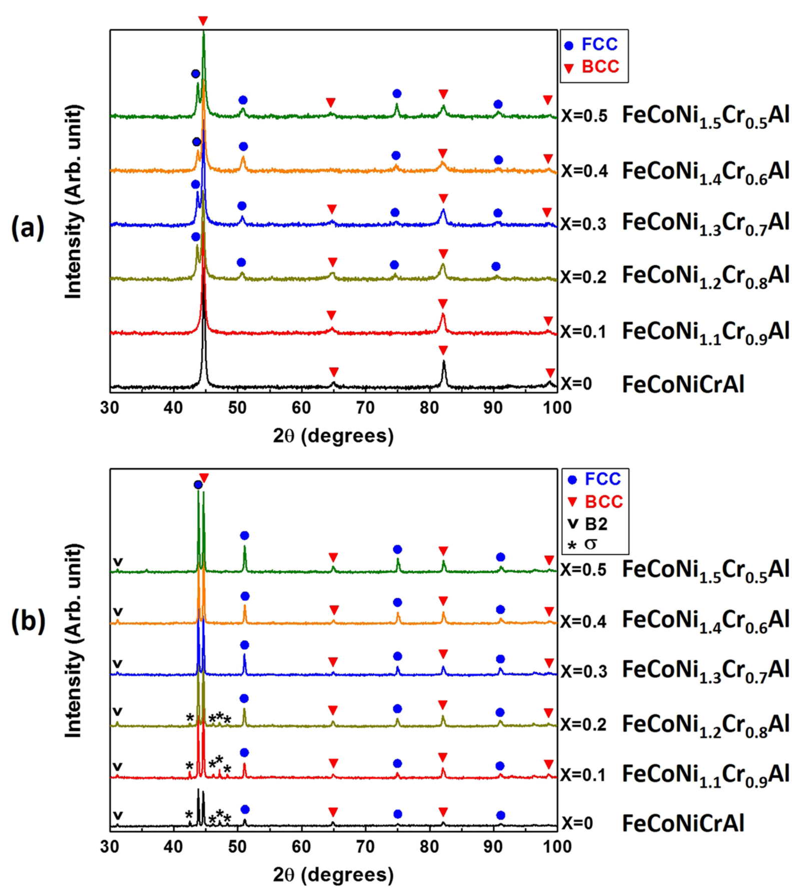

FIG. 1. X-ray diffraction (XRD) patterns of $FeCoNi_{1+X}Cr_{1-X}Al$ HEAs (X=0.0-0.5); (a) as-cast and (b) annealed at 800 °C.

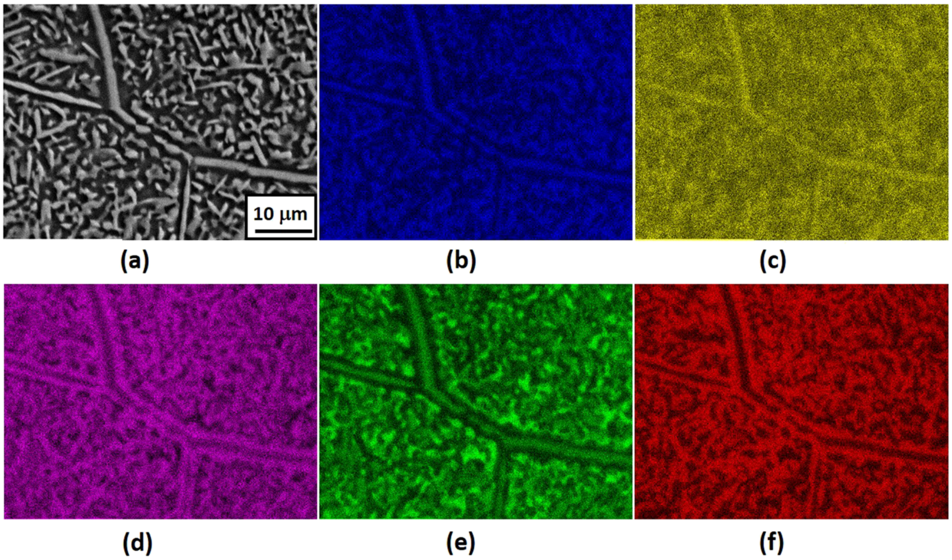

FIG. 2. Microstructural and compositional analysis of FeCoNiCrAl annealed at 1,000 °C: (a) SEM image and (b)-(f) EDS compositional maps of Fe, Co, Ni, Cr and Al elements, respectively, corresponding to (a).

III. RESULTS AND DISCUSSION

Crystallographic phase changes were systematically examined by varying the contents of Ni, Cr and Al elements. Figure 1 shows XRD patterns for the $FeCoNi_{1+X}Cr_{1-X}Al$ HEAs, where Fe, Co, and Al remain constant at 20 at.%. The Ni content increases from 20 at.% (X=0) to 30 at.% (X=0.5), while the Cr decreases to 10 at.% (X=0.5). By comparing peak intensities, the as-cast $FeCoNi_{1+X}Cr_{1-X}Al$ HEAs exhibit a dominant BCC phase with a relatively low portion of FCC phase; only the BCC phase was observed at the equiatomic (X=0) and near equiatomic (X=0.1) FeCoNiCrAl HEAs.

After annealing the as-cast HEAs at 800 °C, the relative integrated intensities of the FCC phase were enhanced and the phase was also found in the compositions of X=0 and 0.1 (as seen in Ref. 14 for 1,000 °C). Such a partial change from BCC to FCC has previously been observed in an equiatomic FeCoNiCrAl HEA over a broad range of annealing temperatures (~600-950 °C), and was attributed to spinodal decomposition, as is also observed in Figure 2.[16–18] After heat treatment at 850 °C, the BCC phase transformed into the σ-FeCr phase, which was also present in the nearly equiatomic compositions of FeCoNiCrAl HEAs. The FeCr-enriched σ phase has been predicted and observed in nearly equiatomic FeCoNiCrAl HEAs annealed at 700 – 1,000 °C, but dissolves into other phases at temperatures higher than 1,000 °C.[16,19] An additional phase was also present at all composition ranges after annealing. This phase is probably ordered (i.e., having a B2 structure) due to the presence of what is likely a {100} reflection, as seen in Fig. 1. Figure 2 shows a disconnected dendrite microstructure composed of BCC and FCC phases and the elemental distribution as determined by EDS mapping.

TABLE I. A summary of structural changes in HEAs of $FeCoNiCr_{1-X}Al_{1+X}$ and $FeCoNi_{1+X}Cr_{1-X}Al$.

			As-cast		Annealed at 800°C	
HEA Type	X amount in HEA	VEC	Structure	Agreement to *VEC*	Structure	Agreement to *VEC*
$FeCoNiCr_{1-X}Al_{1+X}$ (Switching Cr with Al)	X=0.0	7.20	BCC	No	BCC/FCC	Yes
	X=0.1	7.14	BCC	No	BCC/FCC	Yes
	X=0.2	7.08	BCC	No	BCC/FCC	Yes
	X=0.3	7.02	BCC	No	BCC	No
	X=0.4	6.96	BCC	No	BCC	No
	X=0.5	6.90	BCC	No	BCC	No
$FeCoNi_{1+X}Cr_{1-X}Al$ (Switching Cr with Ni)	X=0.0	7.20	BCC	No	BCC/FCC	Yes
	X=0.1	7.28	BCC	No	BCC/FCC	Yes
	X=0.2	7.36	BCC/FCC	Yes	BCC/FCC	Yes
	X=0.3	7.44	BCC/FCC	Yes	BCC/FCC	Yes
	X=0.4	7.52	BCC/FCC	Yes	BCC/FCC	Yes
	X=0.5	7.60	BCC/FCC	Yes	BCC/FCC	Yes

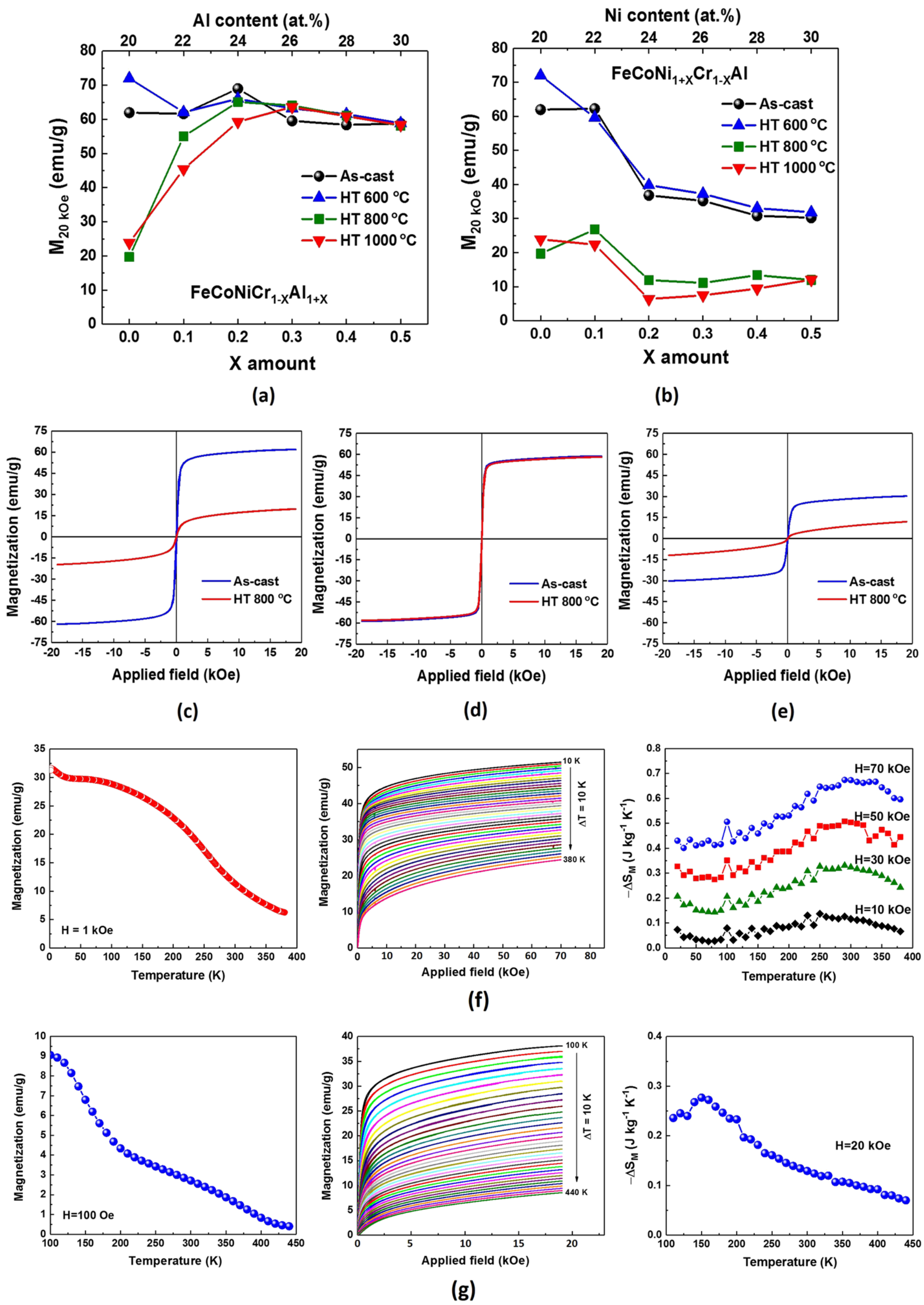

FIG. 3. Magnetic properties measured at room and low temperatures: (a)-(b) Room temperature magnetization measured at 20 kOe ($M_{20\,kOe}$) as a function of subsequent annealing temperatures in FeCoNiCr$_{1\text{-}X}$Al$_{1+X}$ and FeCoNi$_{1+X}$Cr$_{1\text{-}X}$Al HEAs, respectively, (c)-(e) Magnetic hysteresis loops of FeCoNiCrAl (c), FeCoNiCr$_{0.5}$Al$_{1.5}$ (d), FeCoNi$_{1.5}$Cr$_{0.5}$Al (e) HEAs for both as-cast and annealed samples (800 °C for 3h), and (f)-(g) Low temperature dependent magnetization, isothermal hysteresis loops and temperature dependence of the magnetic entropy change of FeCoNiCrAl and FeCoNi$_{1.5}$Cr$_{0.5}$Al HEAs (both annealed at 800 °C), respectively, measured using an MPMS and a VSM.

The typical dendritic structure was well developed in the as-cast condition, but grew and became more disconnected during heat treatment, as seen previously.[17] The elements of Ni and Al are enriched in the matrix BCC phase that correspond to the dark area in Fig. 2(a), while Fe, Co and Cr are dominant in the FCC phase (the bright area). The composition maps of Fe and Cr elements are especially clear and well matched to each other, although composition variations are more pronounced in the Cr than in the Fe map. The crystal structures of as cast and annealed FeCoNiCr$_{1\text{-}X}$Al$_{1+X}$ HEAs were similarly analyzed using XRD; the general phase determination is summarized in Table I.

The possible phases in HEAs can be phenomenologically predicted by VEC which is the number of total electrons accommodated in the valence band including *s*-, *p*- and *d*-electrons.[20] The VEC is defined as $\sum_{i=1}^{n} c_i(VEC)_i$, where $(VEC)_i$ is the VEC for the individual element, and c_i is the concentration of that element. It has been previously observed that only the FCC phase exists at VEC ≥ 8.0, a mixture of FCC and BCC exists at 6.87 ≤ VEC < 8.0, and solely the BCC phase at VEC < 6.87 in HEAs.[21] Here, all $FeCoNi_{1+X}Cr_{1-X}Al$ and $FeCoNiCr_{1-X}Al_{1+X}$ HEAs are assigned to the dual phase region according to the proposed rule for solid solution formation by the VEC, as shown in Table I. The $FeCoNi_{1+X}Cr_{1-X}Al$ HEAs were well matched with the VEC phase determination, but $FeCoNiCr_{1-X}Al_{1+X}$ HEAs mostly show disagreement.

In order to examine the effects of thermal processing on magnetic properties, hysteresis loops were measured as a function of composition and annealing temperature, as shown in Fig. 3. Magnetization values were measured at 20 kOe ($M_{20\,kOe}$) for comparison between samples, and are higher than 58 emu/g for all compositions in the as-cast $FeCoNiCr_{1-X}Al_{1+X}$ HEAs, due to the presence of a ferromagnetic BCC phase. Samples above X=0.3 have $M_{20\,kOe}$ which are independent of the current annealing temperatures (up to 1,000 °C), indicating that the stability of the BCC phase might be enhanced as the Al content increases. In contrast, there are large differences in $M_{20\,kOe}$ when varying annealing temperatures for the FeCoNiCrAl base alloy, due to the partial transformation from BCC to FCC. This results in a reduction of $M_{20\,kOe}$ from 62 emu/g (as-cast) to 20 emu/g (800 °C Anneal). The hysteresis loops clearly show the different magnetic behaviors for FeCoNiCrAl (X=0) and $FeCoNiCr_{0.5}Al_{1.5}$ (X=0.5) HEAs in Fig. 3(c)–(d). Assuming the FCC phase is fully paramagnetic, we can estimate the phase change from the $M_{20\,kOe}$ values between as-cast and annealed samples. A simple calculation for the Cr/Al switching case comparing the as-cast and annealed magnetization values indicates an FCC weight percentage of 14%, 27% and 68% for X=0.2, 0.1, 0, respectively, showing a similar trend with the peak intensity ratio of FCC and BCC phases in the XRD data. We will examine the magnetic properties for each phase using magnetic force microscopy (MFM) and tunnel diode oscillation (TDO) methods in a future study.

Unlike the magnetic behaviors of the $FeCoNiCr_{1-X}Al_{1+X}$ HEAs, $FeCoNi_{1+X}$ $Cr_{1-X}Al$ HEAs are very sensitive to elemental substitutions in the as-cast condition, resulting in the decrease of $M_{20\,kOe}$ with an increase of the Ni content, as shown in Fig. 3(b). As expected from the XRD data in Table I, the value of $M_{20\,kOe}$ steeply drops from 62.2 emu/g (X=0.1, 22 at.% Ni) to 36.8 emu/g (X=0.2, 24 at.% Ni) because of the introduction of the FCC phase in the BCC matrix. Thereafter, it slowly decreases down to 30.2 emu/g at X=0.5 which corresponds to 30 at.% Ni and 10 at.% Cr. After a subsequent anneal at 800 °C, all samples were not magnetically saturated even at an applied field of 20 kOe and the magnetization values at 20 kOe are much lower than those of the as-cast samples; an example can be seen in Fig. 3(e). This can be correlated to a transformation from the ferromagnetic BCC phase to the FCC phase, as was seen in the XRD results in Fig. 1(b). From these results, the $FeCoNi_{1+X}Cr_{1-X}Al$ HEAs may be good candidates for controlling the magnetization value by substitution and annealing processes.

The temperature-dependent magnetic behavior of FeCoNiCrAl and $FeCoNi_{1.5}Cr_{0.5}Al$ HEAs annealed at 800 °C were measured; these samples showed a low magnetization at room temperature, and could be potentially useful for magnetocaloric applications. Figure 3(f)–(g) shows the temperature dependence of magnetization, isothermal hysteresis loops and the temperature dependence of the magnetic entropy for both HEAs. A very broad magnetic phase transition from 100 K to 350 K was observed in the FeCoNiCrAl alloy. In the case of $FeCoNi_{1.5}Cr_{0.5}Al$, there was a first phase transition around 150 K attributed to the FCC phase, then the magnetization slowly decreased toward zero magnetization around 450 K. The hysteresis loops were obtained in the temperature ranges of 10-380 K and 100-440 K, respectively, as shown in the middle figures of Fig. 3(f)–(g). From these isothermal magnetization curves, the magnetic entropy changes (ΔS_M) were calculated using Maxwell's relation:

$$\Delta S_M = \int_0^H \left(\frac{\partial M(H,T)}{\partial T}\right)_H dH \tag{1}$$

The values of (ΔS_M) are found to be negative, with a peak entropy change of $-\Delta S_M$ = 0.674 J·kg^{-1}·K^{-1} at 290 K and an applied field of ~70 kOe for the FeCoNiCrAl, and a peak entropy change of $-\Delta S_M$ = 0.277 J·kg^{-1}·K^{-1} at 150 K and 20 kOe for the $FeCoNi_{1.5}Cr_{0.5}Al$ sample; this temperature is much lower than that for the FeCoNiCrAl alloy (290 K). While small in value, the broad magnetic entropy change centered near RT, as seen in the FeCoNiCrAl alloy, may lead to large refrigerant capacity (RC), which is a measure of the energy that can be transferred between high and low temperatures. RC was estimated by taking the full width at half maximum of the peak in $-\Delta S_M$, corresponding to $RC_{FWHM} = |\Delta S_M^{Peak}| \times \delta T_{FWHM}$. The RC values of 119.2 and 242.6 J·kg^{-1} at 30 and 70 kOe in the annealed FeCoNiCrAl, respectively, are higher than that of Fe-Tm-B-Nb metallic glasses with T_C = 325 K (RC_{FWHM} = 57 J·kg^{-1} at 15 kOe) although the observed value in $-\Delta S_M$ is somewhat lower than that in the metallic glasses, 0.87 J·kg^{-1}·K^{-1} at 325 K.[8] High-entropy metallic glasses (HEMG) such as HoErCoAlX (X=Gd, Dy, and Tm) show high $|\Delta S_M^{Peak}|$ of 11.2-15.0 J·kg^{-1}·K^{-1} and RC_{FWHM} of 375-627 J·kg^{-1} at 50 kOe, but T_C is too low to be used at ambient temperature, ranging from 9-37 K.[2]

IV. CONCLUSIONS

The partial substitution of Ni/Al for Cr in FeCoNiCrAl-type HEAs was investigated, and thermomagnetic and magnetocaloric properties were measured after various thermal anneals. The $FeCoNi_{1+X}Cr_{1-X}Al$ HEAs matched with the VEC model, exhibiting the coexistence of FCC and BCC phases for both the as-cast and annealed conditions. Magnetic properties were significantly affected by increases in the phase percentage of the FCC phase, which is strongly related to both elemental substitution and the annealing condition. The $M_{20\,kOe}$ of $FeCoNi_{1+X}Cr_{1-X}Al$ HEAs are sensitive to both composition and annealing condition, showing a range of 6.6 – 72.0 emu/g. The annealed FeCoNiCrAl HEA shows a maximum value of magnetic entropy change around room temperature and increased refrigerant capacity values due to a broad magnetic entropy change.

ACKNOWLEDGMENTS

This work was funded by the In-House Laboratory Independent Research (ILIR) program for the Force Protection Program of the Office of Naval Research, Program Element 0602123N, managed by the NSWC Carderock Division Director of Research. The authors would like to thank Danielle Gerstner (Naval Surface Warfare Center, Carderock Division) for her assistance with the XRD measurements.

REFERENCES

[1]J. Huo, J.-Q. Wang, and W.-H. Wang, J. Alloys Compd. **776**, 202 (2019).
[2]J. Huo, L. Huo, J. Li, H. Men, X. Wang, A. Inoue, C. Chang, J.-Q. Wang, and R.-W. Li, Journal of Applied Physics **117**, 073902 (2015).
[3]J. T. Huo, L. S. Huo, H. Men, X. M. Wang, A. Inoue, J.-Q. Wang, C. T. Chang, and R. W. Li, Intermetallics **58**, 31 (2015).
[4]Q. Luo and W. H. Wang, J. Alloys Compd. **495**, 209 (2010).
[5]C. Mayer, B. Chevalier, and S. Gorsse, J. Alloys Compd. **507**, 370 (2010).
[6]P. Yu, J. Z. Zhang, and L. Xia, Intermetallics **95**, 85 (2018).
[7]X. C. Zhong, H. C. Tian, S. S. Wang, Z. W. Liu, Z. G. Zheng, and D. C. Zeng, J. Alloys Compd. **633**, 188 (2015).
[8]J. Li, J. Y. Law, H. Ma, A. He, Q. Man, H. Men, J. Huo, C. Chang, X. Wang, and R.-W. Li, J. Non-Crystalline Solids. **425**, 114 (2015).
[9]Y. K. Fang, C. C. Yeh, C. C. Hsieh, C. W. Chang, H. W. Chang, W. C. Chang, X. M. Li, and W. Li, Journal of Applied Physics **105**, 07A910 (2009).
[10]M. S. Lucas, D. Belyea, C. Bauer, N. Bryant, E. Michel, Z. Turgut, S. O. Leontsev, J. Horwath, S. L. Semiatin, M. E. McHenry, and C. W. Miller, Journal of Applied Physics **113**, 17A923 (2013).
[11]M. Kurniawan, A. Perrin, P. Xu, V. Keylin, and M. McHenry, IEEE Magnetics Letters **7**, 6105005 (2016).
[12]J. W. Yeh, S. K. Chen, S. J. Lin, J. Y. Gan, T. S. Chin, T. T. Shun, C. H. Tsau, and S. Y. Chang, Advanced Engineering Materials **6**, 299 (2004).
[13]D. B. Miracle and O. N. Senkov, Acta Materialia **122**, 448 (2017).
[14]S. M. Na, J. H. Yoo, P. K. Lambert, and N. J. Jones, AIP Advances **8**, 056412 (2017).
[15]C. Mayer, S. Gorsse, G. Ballon, R. Caballero-Flores, V. Franco, and B. Chevalier, Journal of Applied Physics **110**, 053920 (2011).
[16]W. R. Wang, W. L. Wang, and J. W. Yeh, J. Alloys Compd. **589**, 143 (2014).
[17]A. Munitz, S. Salhov, S. Hayun, and N. Frage, J. Alloys Compd. **683**, 221 (2016).
[18]W. H. Liu, Y. Wu, J. Y. He, Y. Zhang, C. T. Liu, and Z. P. Lu, J. Metals **66**, 1973 (2014).
[19]T. M. Butler and M. L. Weaver, J. Alloys Compd. **691**, 119 (2017).
[20]U. Mizutani, *Hume-Rothery Rules for Structurally Complex Alloy Phases* (CRC Press, Boca Raton, 2011).
[21]S. Guo, C. Ng, J. Lu, and C. T. Liu, Journal of Applied Physics **109**, 103505 (2011).